Magnetic Field Measurements of First Pre-series Full-Length 4.2 m Quadrupole MQXFA03 Using PCB Rotating Coils for the Hi-Lumi LHC Project

H. Song, *Senior Member, IEEE,* G. Ambrosio, K. Amm, M. Anerella, G. Apollinari, D. Cheng, G. Chlachidze, J. DiMarco, S. Feher, P. Ferracin, S. Izquierdo Bermudez, A. Jain, P. Joshi, J. Muratore, H. Pan, G. Sabbi, J. Schmalzle, E. Todesco, P. Wanderer, X. Wang and M. Yu

***Abstract*—The U.S. Hi-Lumi LHC Accelerator Upgrade Project (AUP) and CERN have joined efforts to develop high field quadrupoles for the Hi-Lumi LHC upgrade. The US national laboratories in the AUP project will deliver 10 magnets and each cryostat has two 4.2 m high gradient quadrupoles in it. These magnets are made of Nb_3Sn conductors, with large aperture (150 mm) and integrated gradient of 556.9 T. This paper reports on magnetic measurements performed during the vertical test at Brookhaven National Laboratory (BNL) in 2019-2020. A warm measurement Z-Scan (+/- 15 A) with 42 Z-positions before cool-down was performed at BNL. The results were directly compared to field data measured at LBNL during magnet assembly. Measured harmonics and magnetic center offsets (ΔX and ΔY) have provided timely and informative diagnostics on the magnet structure's shape at both warm and cold temperatures. A new centering fixture was designed and added to better center the warm bore tube which contains the rotating coil probe. After the quench training to 16.47 kA was achieved, a complete set of cold measurements (Z-Scan at 16.47 kA and I-Scan from 960 A to 16.47 kA and back to 960 A) was made. Periodic axial variation of allowed and nonallowed harmonics was observed which is related to the coil radial and/or mid-plane variations along the magnet axis. Overall, the average harmonics in the straight section are within the required field boundaries.**

***Index Terms*— US AUP, Hi-Lumi LHC, Nb_3Sn, Superconducting magnets, Magnetic Measurements, Z-Scan, DC-Loop (I-Scan), Field Harmonics, Rotating Coil.**

I. Introduction

THE U.S. Hi-Lumi LHC Accelerator Upgrade Project (AUP) and CERN have joined efforts to develop high field quadrupoles for the Hi-Lumi LHC upgrade [1]. The US national laboratories in the AUP project (BNL, FNAL and LBNL) will deliver 10 cryostats of magnets and each cryostat has two 4.2 m high gradient quadrupoles [2]. These magnets are made of Nb_3Sn 40-strand cable with a stainless-steel core. They have large aperture (150 mm) and integrated gradient of 556.9 T [3, 4]. All the component quadrupoles will be tested individually at the vertical superconducting magnet test facility at BNL before assembling and testing the final cold masses at Fermilab [5].

Magnetic field measurement is an important part of magnet testing to ensure that the magnetic field meets the functional requirements and acceptance criteria [6-8]. Feedback from these measurements and analysis has been used to confirm and/or enhance the present design and fabrication process. The new magnetic measurements system has been developed specifically for the MQXFA vertical test [9]. The results are compared with those of short models previously tested in the US and at CERN, and with the warm measurements performed during assembly at LBNL [8]. Recently, the MQXFA03 magnet has achieved the 16.47 kA current target after 10 training quenches in the first thermal cycle. A few typical measurements have been successfully performed including longitudinal Z-Scans at warm temperature and at nominal current after cool-down, and a stair-step measurement (DC Loop), also named I-Scan. It is the first magnet completely fabricated by AUP and is the first pre-series high gradient quadrupole of the MQXF design for the HL-LHC Q1 and Q3 final focus quadrupoles and will be part of the first MQXFA cryo-assembly suitable for operation in the LHC. Primary field measurement results will be reported in the following.

II. Experimental Methods and Setup

The magnetic measurements for the AUP MQXFA magnets have employed two rotating coil probes residing on Printed Circuit Boards (PCB). The use of PCBs technique has been validated – particularly in the HQ magnetic measurement program [7, 10]. The PCB based rotating coil has been successfully used in the MQXAP02 magnet measurement [9]. The rotating coil has two probe coils 220 and 110 respectively, named by their actual lengths, with 220 mm and 110 mm distance from center-to-center location on the PCB.

The magnetic field in the aperture of the straight section of a quadrupole magnet can be expressed in terms of field coefficients in a series expansion in the following complex function formalism [11, 12]:

Manuscript receipt and acceptance dates will be inserted here. This work was supported in part by the U.S. Department of Energy, Office of Science, Office of High Energy Physics, through the U.S. LHC Accelerator Research Program, and in part by the High Luminosity LHC project at CERN. (*Corresponding author: Honghai Song.*)

H. Song, Stony Brook University, Stony Brook, NY 11794, USA, (e-mail: honghai.song@stonybrook.edu and honghaisong@gmail.com).

K. Amm, M. Anerella, P. Joshi, J. Muratore, J. Schmalzle, P. Wanderer, Brookhaven National Laboratory, Upton, NY 11973 USA.

G. Ambrosio, G. Apollinari, G. Chlachidze, J. DiMarco, S. Feher, M. Yu, Fermi National Accelerator Laboratory, Batavia, IL 60510 USA.

D. Cheng, P. Ferracin, H. Pan, G. Sabbi, X. Wang, Lawrence Berkeley National Laboratory, Berkeley, CA 94720 USA.

S. Izquierdo Bermudez, E. Todesco, CERN, Geneva 23, Switzerland.

A. Jain, Argonne National Laboratory, Lemont, IL 60439, USA

Digital Object Identifier will be inserted here upon acceptance.

This document was prepared by LARP collaboration using the resources of the Fermi National Accelerator Laboratory (Fermilab), a U.S. Department of Energy, Office of Science, HEP User Facility. Fermilab is managed by Fermi Research Alliance, LLC (FRA), acting under Contract No. DE-AC02-07CH11359.

This article has been accepted for publication in a future issue of this journal, but has not been fully edited. Content may change prior to final publication. Citation information: DOI 10.1109/TASC.2021.3053510, IEEE Transactions on Applied Superconductivity

$$B_y + iB_x = \sum_{n=1}^{\infty}(B_n + iA_n)(x+iy)^{n-1} = 10^{-4}B_2\sum_{n=1}^{\infty}(b_n + ia_n)(\frac{x+iy}{R_{ref}})^{n-1} \quad (1)$$

where B_x and B_y are the horizontal and vertical field components in T in Cartesian coordinates, B_n and A_n are the normal and skew multipole fields at the reference radius (R_{ref}) of 50 mm. The normal and skew harmonics b_n and a_n in units of 10^{-4} are B_n and A_n normalized to B_2 which is the main field component.

Fig. 1 shows the magnet orientation in the test facility. The powering convention results in a negative normal quadrupole. Per discussions with colleagues at CERN, Fermi Lab and BNL, it has been agreed that, transfer function (TF) reported

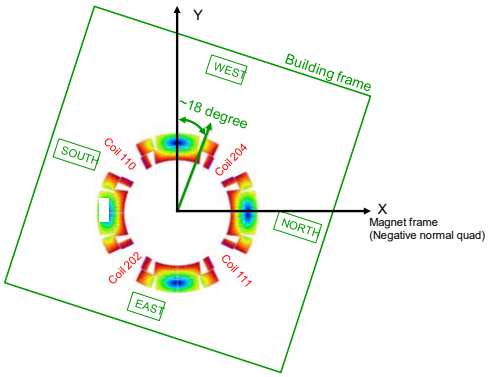

Fig. 1. The orientation of a MQXFA magnet located in the underground Dewar in the vertical testing facility with regards to the building frame (green square) at BNL, powered based on the power convention as defined during the magnet design and fabrication. It has four AUP coils including coils 204, 110, 202, 111, fabricated by BNL and FNAL. The color in the coil block is for the absolute magnetic field strength |*B*|, the rainbow colors from red to blue corresponding to fields from high to low.

as an absolute value. The main field B_2 will be reported as negative to be consistent with the magnet actual coordinate system and polarity, and harmonic coefficients will be normalized to this (negative) B_2. Note that this will leave b_2=+10000. Note that also all the reported harmonics are corrected after the centering and rotation correction process. The centering process calculates the center offsets based on the measured dipole field, and then rotate it to an absolute normal quadrupole and force A_2 to be zero.

The quench training on MQXFA03 was successfully performed and reached 16.67 kA in November. This allowed us to perform a complete set of magnetic field measurements for the first time. All the measurements are summarized in TABLE I including warm Z-Scans, cold Z-Scans at fixed currents and I-Scan at fixed location, as well as ramp rate studies [9]. For all the high current measurements (10 kA and 16.47 kA), the magnet needs to be prepared with a pre-cycle. For the Z-Scan at the nominal current 16.47 kA, measurement steps are 27.185 mm at the magnet ends and 108.74 mm in the straight section. Starting from the non-lead end, the last point was targeted at 4403.97 mm for MQXFA03.

TABLE I
MAGNETIC FIELD MEASUREMENT LOCATIONS AND CURRENTS ON MQXFA03

Qu#	Meas	T(K)	Zpos#	# of Currents, and its pattern	
1	Z-Scan	~300	40	2	+/- 15 A
2	Z-Scan	~300	40	2	+/- 15 A
3	Z-Scan	200	40	2	+/- 18 A
4	Z-Scan	100	40	2	+/- 30 A
7	Z-Scan	1.9	9	1	10 kA
9	Z-Scan	1.9	9	1	960 A
10	I-Scan	1.9	1	23	960A→10kA→960A
14	Z-Scan	1.9	80	1	16.47 kA
16	I-Scan	1.9	1	37	960A→10kA→960A

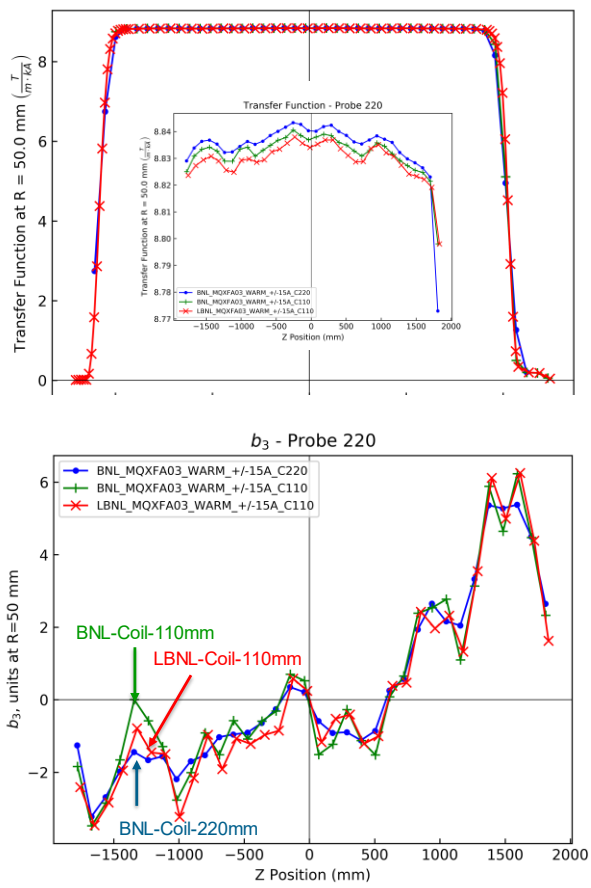

Fig. 2. Warm field measurement comparison between BNL and LBNL. Positive values of z are nearer the lead end of the magnet. Upper: Transfer functions (TF) of Z-Scan as a function of Z position along the magnet axis. Lower: harmonics b_3.

III. MEASUREMENT RESULTS

A. *Warm and cold (low current) measurement at >30 K*

Warm magnetic measurement of magnet MQXFA03 was carried out before the first thermal cool-down at BNL. All the field harmonics of b_n and a_n have been analyzed up to n = 15. Fig. 2 (Upper) presents the TF as function of z positions. In zoom-in figure, all TF are around 8.84 T/(m·kA) are about 2% higher than design value [13]. Harmonics measured at BNL and LBNL have been thoroughly compared and they agree with each other. Harmonic $\boldsymbol{b_3}$ is compared in Fig. 2 (Lower) to BNL's Coil-220 and Coil-110 coil, and LBNL's Coil 110. Overall, BNL's warm measurement results agree with the warm measurement results at LBNL made during magnet as-

This article has been accepted for publication in a future issue of this journal, but has not been fully edited. Content may change prior to final publication. Citation information: DOI 10.1109/TASC.2021.3053510, IEEE Transactions on Applied Superconductivity

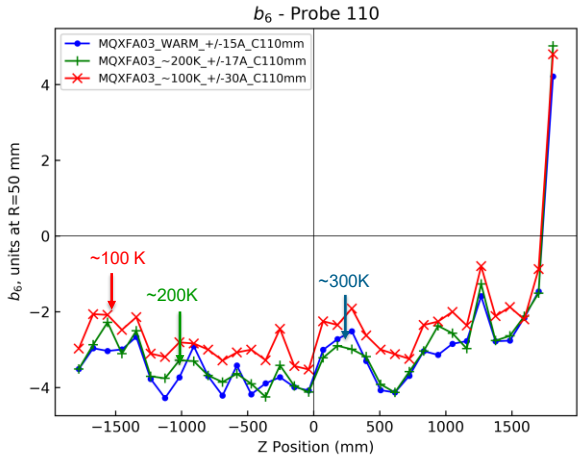

Fig. 3. Temperature dependence of harmonic b_6 in the low current Z-Scan during cool-down from 300 K to 50 K.

sembly. BNL's Coil-110 is shorter which allows it to see more variations along the magnet axis than Coil-220.

Furthermore, more low-current measurements at approximately 300 K, 200 K and 100 K were taken during the cool-down at 15 A, 17 A and 30 A respectively. Note that NLE temperature is lower than that at the lead end (LE) with maximum temperature difference less than 50 K. The allowed b_6 based on the 110 mm probe reading becomes smaller when temperature decreases from 300 K to 100 K as illustrated in Fig.3. Since the magnet temperature is still higher than conductor T_c, no magnetization is involved yet, so it is likely due to the geometrical changes in coils during thermal cooling and shrinkage. Such temperature dependence may be further studied with simulation and modeling.

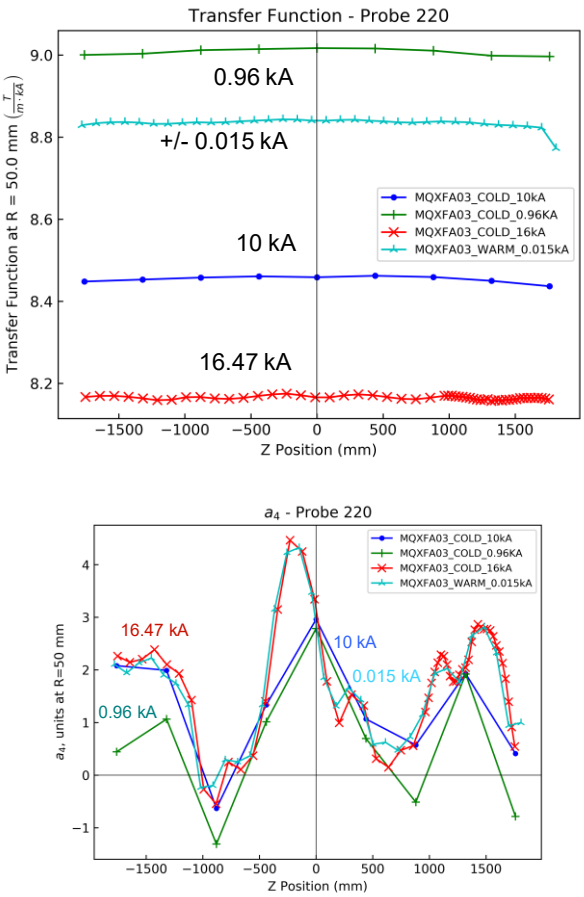

Fig. 4. Transfer functions of all the Z-Scan cases, including +/- 15 A, 960 A, 10 kA and 16.47 kA.

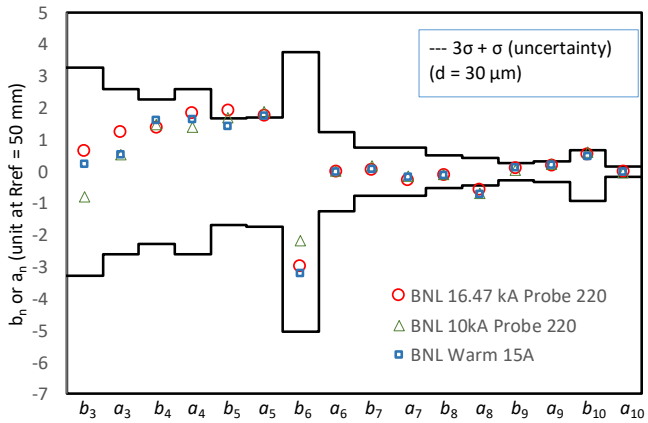

Fig. 5. Averaged harmonics in the straight section, 0.015 kA, 10 kA and 16.47 kA. The upper and lower boundary are for the estimated field harmonics with 3σ geometrical variations and 1σ uncertainty.

B. Cold (high current) Z-Scan at 1.9 K

After the magnet was cooled down to 1.9 K, two "light" versions of Z-Scan field measurements were performed at 960 A and 10 kA before quench tests. There are only 9 positions around the magnet center point with 440 mm increments: 0, +/- 440, +/-880, +/-1320, +/-1760 mm. These Z-Scans have basic field quality information at intermediate gradients before quench tests. After a series of quench tests at 1.9 K, the magnet reached the reference current of 16.47 kA, so was ready for standard versions of Z-Scan and I-Scan. A complete Z-Scan with 84 positions at 16.47 kA at 1.9 K has been made. All the harmonics of b_n and a_n for n up to 15 have been processed with centering and rotation. All four cases of TF and a_4 versus Z positions are plotted in Fig. 4 (Upper) including warm measurement +/-15A, 960 A, intermediate 10 kA, and 16.47 kA measurements. The 960 A measurement has the highest TFs at ~9.0 T/(kA·m), while the 16.47 kA has the lowest TFs at 8.15 T/(kA·m), which is due to the iron saturation. Note that the warm measurement has 42 z-positions with steps of 108.74 mm, 960 A and 10 kA intermediate currents have only 9 Z-positions with step of 440 mm, and 16.47 kA measurement has 84 z-positions with finer steps of 27.185 mm at the magnet ends, but 108.74 mm step in straight sections.

This article has been accepted for publication in a future issue of this journal, but has not been fully edited. Content may change prior to final publication. Citation information: DOI 10.1109/TASC.2021.3053510, IEEE Transactions on Applied Superconductivity

Nonallowed harmonics a_4 are compared within the four measurements as shown in Fig. 4 (Lower). The 9-points measurements at 960 A and 10 kA before the quench training started, fall on the measurement profiles of 15 A (warm) and 16.47 kA (cold) which have 84 z-positions measurements. The 960 A profile is slightly lower than the other three particularly at magnet ends which is likely related to superconducting magnetization. One of the most outstanding phenomena Fig. 4 (Lower) is the periodic variation (wiggles) along the z-axis particularly for the 16.47 kA measurement. It is most likely due to the Nb_3Sn cumferential direc cussion section.

TABLE II
AVERAGED NORMAL AND SKEW HARMONICS (STRAIGHT SECTION) AND RMS OF MQXFA03

bn/an	+/- 15A		960 A		10 kA		16.47 kA	
Temp	Warm		1.9 K		1.9 K		1.9 K	
	Ave	RMS	Ave	RMS	Ave	RMS	Ave	RMS
b_3	0.25	2.38	2.58	3.32	-0.80	2.06	0.67	2.73
a_3	0.54	2.11	0.05	2.12	0.54	2.45	1.26	1.96
b_4	1.62	2.12	1.46	2.37	1.48	2.76	1.39	2.07
a_4	1.64	1.13	0.76	1.26	1.41	1.61	1.86	1.02
b_5	1.45	0.95	1.17	1.24	1.70	1.84	1.93	1.03
a_5	1.77	0.83	1.61	1.63	1.91	1.84	1.78	1.04
b_6	-3.19	0.67	-15.49	15.50	-2.17	2.25	-2.98	0.73
a_6	0.01	0.61	-0.04	0.47	0.04	0.56	0.00	0.57
b_7	0.09	0.30	0.50	0.60	0.20	0.35	0.08	0.29
a_7	-0.17	0.39	0.16	0.40	-0.13	0.37	-0.24	0.39
b_8	-0.11	0.22	-0.16	0.33	-0.08	0.23	-0.09	0.19
a_8	-0.69	0.32	-0.92	0.87	-0.67	0.67	-0.54	0.41
b_9	0.12	0.15	-0.11	0.20	0.06	0.16	0.11	0.16
a_9	0.21	0.16	0.23	0.22	0.23	0.22	0.21	0.17
b_{10}	0.48	0.16	3.20	3.20	0.62	0.63	0.55	0.15
a_{10}	0.00	0.12	0.02	0.14	-0.01	0.14	0.01	0.15

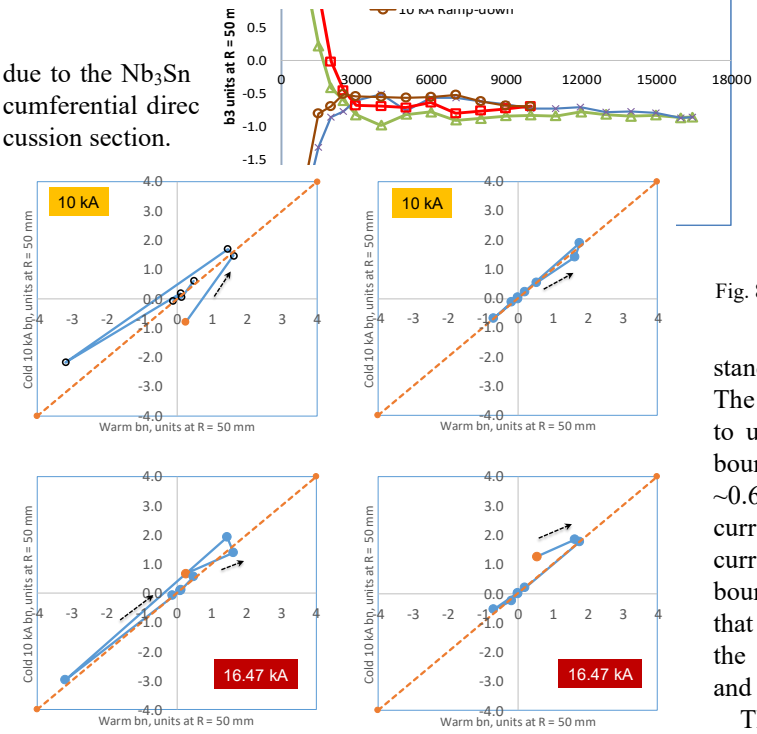

Fig. 6. Linear correlation check between cold (10 kA and 16.47 kA) and warm harmonics (15 A). The yellow dot is the first point for b_3 or a_3. The arrow indicates the sequence of harmonics with n up to 10. The dashed line has a slope of 1.

Harmonics b_n and a_n ($3 \le n \le 10$) in the straight section and their RMS in the range of -1.7 m to 1.7 m around the magnet longitudinal midpoint are averaged and summarized in Table II. It compares four typical measurements of the high current 16.47 kA, intermediate 10 kA and 960 A, and low current +/- 15 A. All averaged harmonics ($3 \le n \le 10$) are plotted in Fig. 5. The upper and lower boundaries are based on the calculated

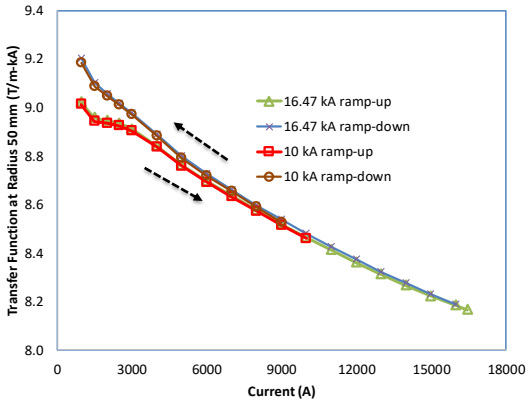

Fig. 7. Two I-Scans of MQXFA03 from 960 A to 10 kA and 16.47 kA, and back to 960 A, at 1.9 K. The red lines are for the 10-kA ramp-up and amp-down. The green and blue lines are for the 16.47 kA ramp up and down.

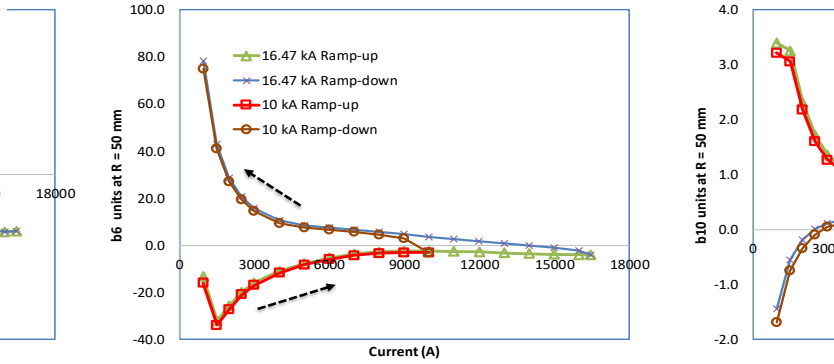

Fig. 8. Allowed harmonics b_6 in I-SCAN of MQXFA03, based on Coil-220.

standard deviation δ due to geometrical variations of 30 μm. The boundary allows for 3δ due to random errors and 1δ due to uncertainty on the systematic when I_{op} = 16.47 kA. The boundaries are slightly different in b_6 due to persistent current, ~0.66 units, but no change for b_{10}. The impact of persistent current in the cable has been considerably reduced at higher currents. All the harmonics are within the upper and lower bounds, except b_5 and a_8 which are slightly larger. It indicates that the magnet does meet the design specification and fulfil the HL LHC's requirements. All the averaged harmonics b_n and a_n where n up to 10 are summarized in Table II.

The averaged harmonics in the warm and cold Z-Scan measurement are correlated in Fig. 6. The averaged harmonics b_n of 10 kA Z-Scan are plotted versus b_n of 15A in the straight sections in the Z-Scan in the upper-left in Fig. 6, and harmonics a_n of 10 kA versus a_n of 15A Z-Scan in Z-Scan in the upper-right in Fig. 6. The yellow dot is for the first point of b_3 or

a_3 when harmonic index n=3, and the rest of dots are against the line with slope = 1. The two plots in the second line are the

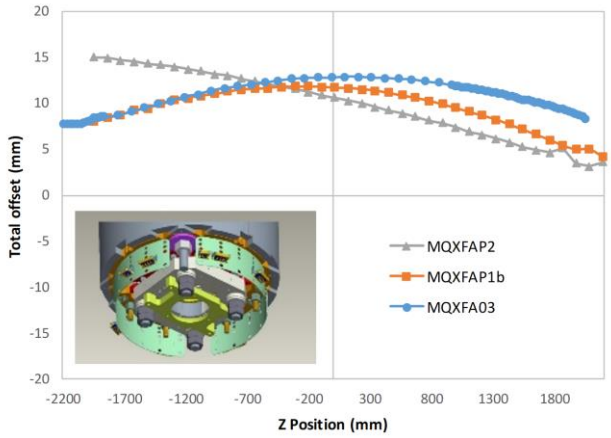

Fig. 9. Measured center offsets (=√(ΔX²+ΔY²) in the Z-Scan measurements for all the three tested magnets MQXFAP2, MQXFAP1b, and MQXFA03, at 16.47 kA and 1.9 K. (Insert: A special centering fixture (dark green) was added to the magnet at the non-lead end (bottom) to center the warm bore tube which contains the rotating PCB coils inside the magnet assembly.)

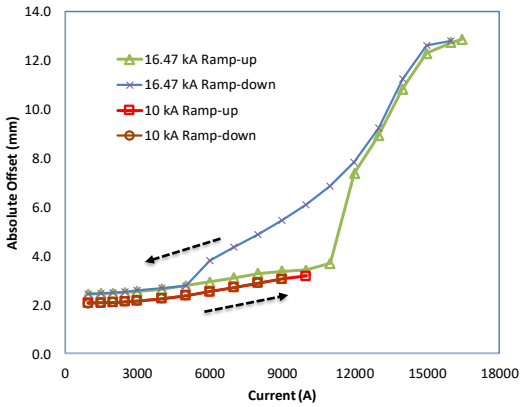

Fig. 10. Measured center offsets (=√(ΔX²+ΔY²) in the Z-Scan measurements for all the three tested magnets MQXFAP2, MQXFAP1b, and MQXFA03, at 16.47 kA and 1.9 K.

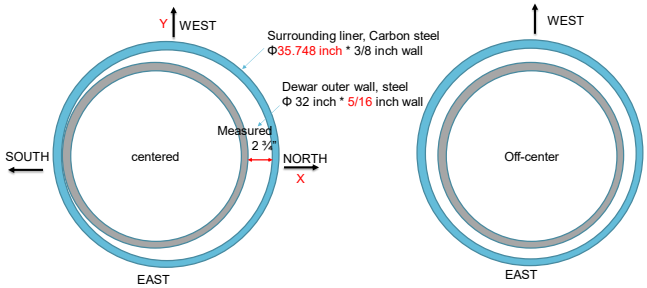

Fig. 11. Off-center (Left) and centered (Right) 2D Sketches to illustrate the relationship between the steel liner (gray circle) and the underground cryostat (blue circle) before and after the 4 spacers were added for the centering correction. The vertical cryostat contains the magnet MQXFA03 cold mass and was hung vertically during the magnet testing. The steel liner is a circular hole, designed to align the vertically Dewar vertically and symmetrically. The liner is off center in the trench hole, with one side touch-ing, and the other side having a 2.75-inch (69 mm) gap. This asymmetry has been corrected by repositioning the cryostat and inserting non-magnetic spacers.

16.47 kA measurement. b_4 and a_3 are slightly off the slope =1 line. Since the individual harmonics a_n and b_n are orthogonal, values for one warm/cold pair are independent of those of any other warm/cold pair. It is possible that a linear relationship exists between the warm and cold measurements. Data from more than one magnet is needed to validate the linear correlation between the cold and warm harmonics.

C. Cold (high current) I-Scan at 1.9 K

I-Scan, also known as "DC-Loop", has been performed to study the current dependence of harmonics when the rotating coil 220 is held at the magnet center location. The 110 mm probe is located 220 mm higher than the 220 mm probe location and signals are recorded at the same time. MQXFA03 has both 10 kA and 16.47 A I-Scan as shown as illustrated in Fig.7. The two I-Scans almost overlap each other when currents are below 10 kA. More hysteresis is observed at low currents; it becomes less when the current is more than 10 kA. The TF decreases from 8.84 T/(m·kA) to 8.2 T/(m·kA) as the current increases from 960 A to 16.47 kA.

Allowed harmonics b_6 and b_{10} and nonallowed harmonics b_3, a_3, a_6 and a_{10} in I-SCANs of MQXFA03 have been analyzed, but only b_6 is presented in Fig. 8 due to its significance up to 60 units at lower current range. Other allowed harmonic a_{10} is less than 3 units and has large hysteresis. The nonallowed harmonics b_3, and a_3 are less than 2 units and the others are less than 0.5 units, though with slight hysteresis. The DC-Loop measurements for the MQXFAP03 are within expectation, similar to the field results of the CERN short MQXF models in [6] and the LARP short magnets in [7].

D. Center offsets in the Z-Scan and I-Scan

Offsets were measured between the magnetic centers and the rotating coil centers. The magnetic centers along the vertical axis depend on both the magnet position extending from the top support flange to the bottom, and the rotating coil position inside the warm bore tube (WBT). Fig. 9 compares the center offsets of three tested magnets, MQXFAP2, MQXFAP1b, and MQXFA03. Note *the* MQXFAP1b *magnet has smaller offsets than* MQXFAP2 *because a centering fixture was added to the* MQXFAP1b *NLE and has constrained the lower end of the warm bore tube (WBT) from moving relatively to the magnet structure.* As a result, the absolute center offset (=√(ΔX²+ΔY²) becomes smaller at the NLE end for the two magnets. The maximum offset magnitude in MQXFAP03 is ~13 mm which is smaller than that in MQXFAP02, and similar to that in MQXFAP1b.

Moreover, magnitudes of the absolute center offsets for the I-Scan when the measurement coils are located at the magnet center regimes (z_{pos} = 0 mm) are displayed in Fig. 10. The ramp up and ramp down are indicated by arrows and colors. The changes of the center offsets with currents are non-linear and shows a large hysteretic behavior. It is important to note that, the total offset in MQXFA03 is ~12 mm at z_{pos} = 0 mm and I = 16.47 kA, which is indeed consistent with the DC-Loop measurement in Fig. 10. Note also that, all the field data has bee processed by the rotation and centering in the data

This article has been accepted for publication in a future issue of this journal, but has not been fully edited. Content may change prior to final publication. Citation information: DOI 10.1109/TASC.2021.3053510, IEEE Transactions on Applied Superconductivity

analysis, so that the center-offsets have been corrected. It's nature to define the magnetic center as the location where the dipole feed down is zero for a quadrupole. The centering process calculates the center offsets based on the measured dipole field, and then rotate it to an absolute normal quadrupole and force A2 to be zero.

After the investigation, it was found that the steel liner of the pit in which the cryostat is installed was off center as shown in Fig. 11. The liner is off center in the trench hole, with one side touching, and the other side having a 2.75-inch (69 mm) gap. This asymmetry has been corrected by repositioning the cryostat and inserting non-magnetic spacers.

IV. Discussions and Analysis

Possible relationship between coil size variations and harmonics variations

In the all the Z-Scans presented before, one of prominent

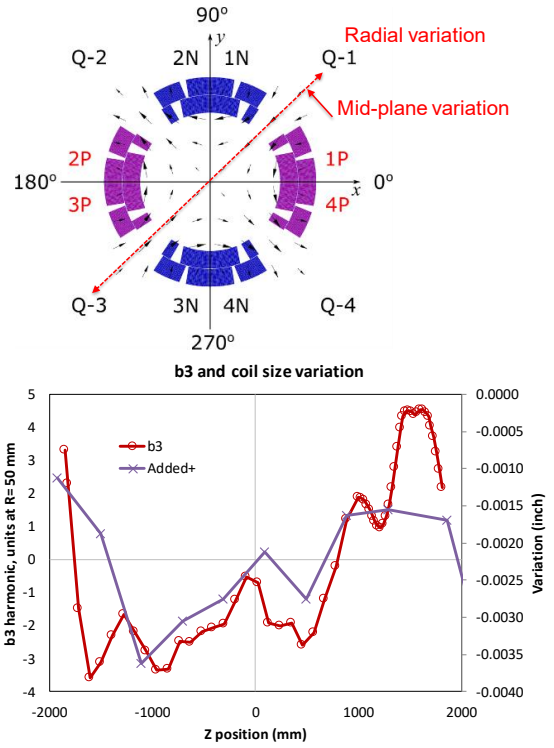

Fig. 12. Radial and mid-plane variations of the AUP MQXFA03 magnet. (1) Illustration of the radial and mid-plane variations K.

behaviors of the b_n and a_n is the "wiggle" variations along the magnetic Z axis. Magnetic field measurement comparison between only the coil pack and the magnet with loading at LBNL[8], has indicated that the wiggles likely come before the coils are loaded inside the shells. Thus, it was traced back to the coil size and its variation, as well as the presence of magnetic pins at connecting the poles of the two coil layers. The pins have been changed to non-magnetic ones in the current coil and magnet production. Holik *et al* studied the coil size variations before but the study was not directly linked to measured harmonics or its variations [14]. In order to find the relationship, Coordinate-measuring machine (CMM) coil size data for the coils used in magnet MQXFA03 were provided by D. Cheng at LBNL [15].

An ideal quad has all the symmetries including top and bottom (TB), left-and right (LR), and quad coil (QC) special symmetry around the coil mid-plane [11]. However, the actual coils have both radial and mid-plane variations as illustrated in in Fig. 12 (Upper). When the coils have radial variations, they will break the TB and LR symmetries, though it is not clear if the QC symmetry is kept or not. When the coils have mid-plane variations, all the TB, LR, and QC symmetries do not apply anymore. With such variations, some zero-harmonics in the ideal quad become nonzero.

The relationship between b_3 and the coil size variation is illustrated and analyzed in Fig. 12 (Lower). Both have larger harmonics at the LE which is consistent with the increase of the added variations of both at the LE. It is likely that both radial and mid-plane variations have contributed to the low order harmonics. If the coil variation measurement by the CMM could have smaller measurement steps and more data points, similar to that of cold measurement at ~110 mm, it will be easier for the comparison and analysis. Another approach is to calculate the field harmonics based on the measured coil size variation and then compare it to the measured one. More studies are needed to better understand the relationship between the harmonic wiggles and coil size variations.

In addition, after the vertical magnet tests (quench training) at BNL, the two pre-series magnet MQXFA03 and 04 will be assembled into a horizontal magnet at FANL. The magnetic field will be re-measured and compared to the BNL's vertical measurements. Both results at BNL and FNAL will be referenced to the future magnet installation and operation at CERN.

V. Conclusion

The quadrupole MQXFA03 is the first quadrupole that will be used in a tunnel-ready cryo-assembly. A complete set of Z-Scan and I-Scan measurements has been successfully achieved along with the successful quench training of MQXFA03. The averaged harmonics in the straight sections are within the 4δ upper and lower boundaries which indicate that the field harmonics meet the design specification and the magnet quality fulfills the Hi-Lumi LHC requirements.

Magnetic field measurement capabilities have been improved in a few aspects. (1) The warm bore tube and rotating coil have been modified and improved to reach the longest distance at the NLE. (2) The new centering fixture has been installed. (3) The underground Dewar has been centered by inserting non-magnetic parts. All these improvements will benefit future magnetic field measurements for the DOE AUP project.

The magnetic field harmonics is one of the most important quality assurance parameters in monitoring the magnet quality from assembly at LBNL to single magnet vertical testing (BNL), to two magnet sets in a cryostat horizontal tests at FNAL, and final installation and operation at CERN.

REFERENCES

[1] G. Apollinari, S. Prestemon, and A. V. Zlobin, "Progress with High-Field Superconducting Magnets for High-Energy Colliders," *Annual Review of Nuclear and Particle Science, Vol 65,* vol. 65, pp. 355-377, 2015.

[2] G. Ambrosio, "Nb3Sn High Field Magnets for the High Luminosity LHC Upgrade Project," *IEEE Transactions on Applied Superconductivity,* vol. 25, no. 3, Jun, 2015.

[3] P. Ferracin, G. Ambrosio, M. Anerella, H. Bajas, M. Bajko, B. Bordini, R. Bossert, N. Bourcey, D. W. Cheng, G. Chlachidze, L. D. Cooley, S. F. Troitino, L. Fiscarelli, J. Fleiter, M. Guinchard, S. I. Bermudez, S. Krave, F. Lackner, F. Mangiarotti, M. Marchevsky, V. Marinozzi, J. Muratore, A. Nobrega, H. Pan, J. C. Perez, I. Pong, S. Prestemon, H. Prin, E. Ravaioli, G. L. Sabbi, J. Schmalzle, S. S. Tavares, S. Stoynev, E. Todesco, G. Vallone, P. Wanderer, X. R. Wang, and M. Yu, "The HL-LHC Low-beta Quadrupole Magnet MQXF: From Short Models to Long Prototypes," *IEEE Transactions on Applied Superconductivity,* vol. 29, no. 5, Aug, 2019.

[4] P. Ferracin, G. Ambrosio, M. Anerella, A. Ballarino, H. Bajas, M. Bajko, B. Bordini, R. Bossert, D. W. Cheng, D. R. Dietderich, G. Chlachidze, L. Cooley, H. Felice, A. Ghosh, R. Hafalia, E. Holik, S. I. Bermudez, P. Fessia, P. Grosclaude, M. Guinchard, M. Juchno, S. Krave, F. Lackner, M. Marchevsky, V. Marinozzi, F. Nobrega, L. Oberli, H. Pan, J. C. Perez, H. Prin, J. Rysti, E. Rochepault, G. Sabbi, T. Salmi, J. Schmalzle, M. Sorbi, S. S. Tavares, E. Todesco, P. Wanderer, X. Wang, and M. Yu, "Development of MQXF: The Nb3Sn Low-beta Quadrupole for the HiLumi LHC," *IEEE Transactions on Applied Superconductivity,* vol. 26, no. 4, Jun, 2016.

[5] J. F. Muratore, K. Amm, M. Anerella, G. Ambrosio, G. Apollinari, M. Baldini, R. H. Carcagno, G. Chlachidze, D. W. Cheng, S. Feher, P. Joshi, P. Kovach, A. Marone, M. Marchevsky, V. Marinozzi, H. Pan, E. Ravaioli, G. Sabbi, H. Song, and P. Wanderer, "Test Results of the First Two Full-Length Prototype Quadrupole Magnets for the LHC Hi-Lumi Upgrade," *IEEE Transactions on Applied Superconductivity,* vol. 30, no. 4, pp. 1-5, 2020.

[6] S. I. Bermudez, G. Ambrosio, H. Bajas, G. Chlachidze, J. F. Troitino, P. Ferracin, L. Fiscarelli, P. Hagen, E. F. Holik, J. Di Marco, S. E. Stoynev, E. Todesco, G. Sabbi, G. Vallone, and X. R. Wang, "Geometric Field Errors of Short Models for MQXF, the Nb3Sn Low-beta Quadrupole for the High Luminosity LHC," *IEEE Transactions on Applied Superconductivity,* vol. 28, no. 3, Apr, 2018.

[7] J. DiMarco, G. Ambrosio, G. Chlachidze, P. Ferracin, E. Holik, G. Sabbi, S. Stoynev, T. Strauss, C. Sylvester, M. Tartaglia, E. Todesco, G. Velev, and X. Wang, "Magnetic Measurements of the First Nb3Sn Model Quadrupole (MQXFS) for the High-Luminosity LHC," *IEEE Transactions on Applied Superconductivity,* vol. 27, no. 4, Jun, 2017.

[8] X. R. Wang, G. E. Ambrosio, D. W. Cheng, G. Chlachidze, J. DiMarco, W. Ghiorso, C. Hernikl, T. M. Lipton, S. Myers, H. Pan, S. O. Prestemon, and G. Sabbi, "Field Quality Measurement of a 4.2-m-Long Prototype Low-beta Nb3Sn Quadrupole Magnet During the Assembly Stage for the High-Luminosity LHC Accelerator Upgrade Project," *IEEE Transactions on Applied Superconductivity,* vol. 29, no. 5, Aug, 2019.

[9] H. Song, J. DiMarco, A. Jain, G. Sabbi, P. Wanderer, and X. Wang, "Vertical Magnetic Measurements of the First Full-Length Prototype MQXFAP2 Quadrupole for the LHC Hi-Lumi Accelerator Upgrade Project," *IEEE Transactions on Applied Superconductivity,* vol. 29, no. 5, pp. 4004707, 2019.

[10] J. DiMarco, G. Ambrosio, M. Anerella, H. Bajas, G. Chlachidze, F. Borgnolutti, R. Bossert, D. Cheng, D. Dietderich, H. Felice, T. Holik, H. Pan, P. Ferracin, A. Ghosh, A. Godeke, A. R. Hafalia, M. Marchevsky, D. Orris, E. Ravaioli, G. Sabbi, T. Salmi, J. Schmalzle, S. Stoynev, T. Strauss, C. Sylvester, M. Tartaglia, E. Todesco, P. Wanderer, X. Wang, and M. Yu, "Test Results of the LARP Nb3Sn Quadrupole HQ03a," *IEEE Transactions on Applied Superconductivity,* vol. 26, no. 4, Jun, 2016.

[11] A. Jain, "Basic theory of magnets." pp. 1-26.

[12] A. Jain, M. Anerella, J. Escallier, G. Ganetis, A. Ghosh, R. Gupta, E. Kelly, A. Marone, G. Morgan, J. Muratore, A. Prodell, W. Sampson, R. Thomas, P. Thompson, P. Wanderer, and E. Willen, "Superconducting 13 cm corrector magnets for the relativistic heavy ion collider (RHIC)," *IEEE Transactions on Applied Superconductivity,* vol. 10, no. 1, pp. 188-191, Mar, 2000.

[13] S. I. Bermudez, L. Fiscarelli, G. Ambrosio, H. Bajas, G. Chlachidze, P. Ferracin, J. DiMarco, S. E. Stoynev, E. Todesco, G. Sabbi, and G. Vallone, "Magnetic Analysis of the MQXF Quadrupole for the High-Luminosity LHC," *IEEE Transactions on Applied Superconductivity,* vol. 29, no. 5, pp. 1-5, 2019.

[14] E. F. Holik, G. Ambrosio, M. Anerella, R. Bossert, E. Cavanna, D. Cheng, D. R. Dietderich, P. Ferracin, A. K. Ghosh, S. I. Bermudez, S. Krave, A. Nobrega, J. C. Perez, I. Pong, G. Sabbi, C. Santini, J. Schmalzle, P. Wanderer, X. R. Wang, and M. Yu, "Fabrication of First 4-m Coils for the LARP MQXFA Quadrupole and Assembly in Mirror Structure," *IEEE Transactions on Applied Superconductivity,* vol. 27, no. 4, Jun, 2017.

[15] D. W. Cheng, G. Ambrosio, E. C. Anderssen, P. Ferracin, P. Grosclaude, M. Guinchard, J. Muratore, H. Pan, S. O. Prestemon, and G. Vallone, "Mechanical Performance of the First Two Prototype 4.5 m Long Nb < sub > 3 </sub > Sn Low-& x03B2; Quadrupole Magnets for the Hi-Lumi LHC Upgrade," *IEEE Transactions on Applied Superconductivity,* vol. 30, no. 4, Jun, 2020.